INVESTIGATION OF THE NUCLEAR STRUCTURE OF THE ISOTOPES $^{170-180}$Os

INVESTIGACIÓN DE LA ESTRUCTURA NUCLEAR DE LOS ISÓTOPOS $^{170-180}$Os

Fatima M. Ali, Mushtaq A. Al-Jubbori*, Rabee B. Alkhayat

Department of Physics, College of Education for Pure Sciences, University of Mosul, 41001 Mosul, Iraq.

(Recibido: Jun./2023. Aceptado: Nov./2023)

Abstract

Interacting Boson Model (IBM-1), Semi Empirical Formula (SEF), and New Empirical Equation (NEE) methods were utilized to determine the energy states of the ground-state (GS), β and γ-bands in the $^{170\text{-}180}$Os isotopes. The results of the study on the GS, β, and γ bands suggest that IBM-1, SEF, NEE, and existing empirical evidence show some agreement, albeit with some discrepancies. The NEE results for GS, β, and γ bands are more reliable with empirical data than the estimates derived from the IBM-1 and SEF models. The reduced transition probabilities B(E2) of the IBM-1 model correspond well to the experimental data. In the GSB, the energies of the 6^+, 8^+, and 10^+ states are not precisely modeled in the IBM-1 model. The $R_{4/2}$ values of low-lying energy levels of Os isotopes fluctuate gradually with increasing neutron numbers. The EPS counter indicates that the transition limit of the $^{170\text{-}180}$Os isotopes has a rotational–vibrational γ-soft transition.

Keywords: IBM-1, SEF, NEE, energy levels, electromagnetic transition.

* mushtaq_phy@uomosul.edu.iq doi: https://doi.org./10.15446/mo.n68.109589

Resumen

Se utilizaron los métodos del modelo de bosones en interacción (IBM-1), la fórmula semiempírica (SEF) y la nueva ecuación empírica (NEE) para determinar los estados energéticos del estado fundamental (GS) y las bandas β y γ en los isótopos $^{170\text{-}180}$Os. Los resultados del estudio para el estado fundamente y para las bandas β y γ sugieren que los métodos IBM-1, SEF, NEE y las pruebas empíricas existentes muestran cierta concordancia, aunque con algunas discrepancias. Los resultados de la NEE para el estado fundamental y para las bandas β y γ son más fiables con los datos empíricos que las estimaciones derivadas de los modelos IBM-1 y SEF. Las probabilidades de transición reducidas B(E2) del modelo IBM-1 corresponden correctamente a los datos experimentales. En el GSB, las energías de los estados 6^+, 8^+ y 10^+ no se modelan con precisión en el modelo IBM-1. Los valores $R_{4/2}$ de los niveles energéticos bajos de los isótopos de Os fluctúan gradualmente con el aumento del número de neutrones. El contador EPS indica que el límite de transición de los isótopos $^{170\text{-}180}$Os tiene una transición rotacional vibracional γ suave.

Palabras clave: IBM-1, SEF, NEE, niveles de energía, transición electromagnética.

Introduction

The properties of different even-even nuclei show variations based on the amount of constituent protons and neutrons, which is associated with the corresponding modifications in the nuclear excitation spectrum and in the decay properties of the stimulated states [1, 2]. The description of the nuclear structure can be studied with numerous tools, one of which is the interacting boson model (IBM-1). Based on algebraic group methods, the Hamiltonians describe the combined nuclear energy properties for a variety of nuclei [3, 4]. IBM-1 is useful in explaining the collective nuclear states of even-even nuclei. The neutrons and protons have not

been differentiated in IBM-1. The nuclear structure is complicated because each nucleon interacts with every other nucleon. The IBM-1 model delineates three groups that are dynamically symmetric, namely the spherical limit U(5), symmetric rotor SU(3), and γ-unstable O(6), in relation to the unitary group U(6) [5–11]. Regan et al. [12] introduced the E-GOS function, which represents the relationship between $E\gamma/I$ as a function of the spin I (E-GOS).

This function has provided valuable insights into the evolution of the yrast line in nuclei. Moreover, they have observed the evolution of the yrast states of numerous nuclei in the $A = 110$ region.

The ratio between the energies of the $I + 2$ and I states is an excellent indicator of properties of the nucleus [13].

Gupta and Sharma [14] investigated the ratio $B(\mathrm{E2}; 4^+ \to 2^+)/B(\mathrm{E2}; 2^+ \to 0^+)$ for even-even Nd-Hg nuclei using the IBM-1 instrument.

Recently, the deformation properties of even-even rare-earth Er-Os nuclei for the number of neutrons $\mathrm{N}_n = 100$ have been studied [15]. These investigations raise the possibility of investigating the deformation properties of Er-Os nuclei for $\mathrm{N}_n = 102$. The isotopes of Os are situated within a region characterized by an abundance of neutrons. On the other hand, it is possible to calculate the nuclear properties of neutron-rich isotopes using other models, such as the shell model. Excitation energies and transition rates for neutron-rich Yb, Hf, W, Os, and Pt isotopes with atomic masses between 180 and 200 are computed using an interacting boson model Hamiltonian derived from Hartree Fock-Bogoliubov calculations with the microscopic Gogny energy density functional D1M [16]. The IBM-1 model was employed to compute the low-lying positive parity yrast bands and B(E2) values in Hf, W, and Os isotopes with $\mathrm{N}_n = 108$ neutrons [17].

The aim of this study is to employ the IBM-1 framework for the purpose of contrasting the computed energy levels, transition probabilities B(E2), and potential energy surfaces of a particular group of even-even $^{170-180}$Os isotopes with those derived from empirical investigations. We performed a comparative analysis of SEF and NEE calculations with empirical and IBM-1 results.

1. Basic calculations

1.1. IBM-with other computations

The key characteristic of the IBM-1 model applies to the bosonic nature of each valence nucleon, with the remaining nucleons constituting the nucleus's inert core. The nucleons have been divided into two distinct components, namely the s-bosons with an angular momentum of $I = 0$ and the d-bosons with $I = 2$. The interaction of bosons results in the formation of the Hamiltonian tensor, which can be characterized as follows.

$$\hat{H} = \sum_{i=1}^{N} \epsilon_i + \sum_{i<j}^{N} V_{ij}, \tag{1}$$

Where ϵ is boson energy, N is the number of bosons, and V_{ij} is the boson–boson interaction.

The IBM-1 Hamiltonian necessitates the consideration of nine distinct factors [18–20].

$$\begin{aligned}\hat{H} =& \epsilon_s \left[s^\dagger \cdot \tilde{s}\right] + \epsilon_d \left[d^\dagger \cdot \tilde{d}\right] + \sum_{L=0,2,4} \frac{1}{2}\sqrt{2L+1} C_L \left[\left[d^\dagger \times d^\dagger\right]^{(L)} \times \left[\tilde{d} \times \tilde{d}\right]^{(L)}\right]^{(0)} + \\ & \frac{1}{\sqrt{2}} \upsilon_2 \left[\left[d^\dagger \times d^\dagger\right]^{(2)} \times \left[\tilde{d} \times \tilde{s}\right]^{(2)} + \left[d^\dagger \times s^\dagger\right]^{(2)} \times \left[\tilde{d} \times \tilde{d}\right]^{(2)}\right]^{(0)} + \\ & \frac{1}{2} \upsilon_0 \left[\left[d^\dagger \times d^\dagger\right]^{(0)} \times \left[\tilde{s} \times \tilde{s}\right]^{(0)} + \left[s^\dagger \times s^\dagger\right]^{(0)} \times \left[\tilde{d} \times \tilde{d}\right]^{(0)}\right]^{(0)} + \\ & \frac{1}{2} u_0 \left[\left[s^\dagger \times s^\dagger\right]^{(0)} \times \left[\tilde{s} \times \tilde{s}\right]^{(0)}\right]^{(0)} + u_2 \left[\left[d^\dagger \times s^\dagger\right]^{(2)} \times \left[\tilde{d} \times \tilde{s}\right]^{(2)}\right]^{(0)}.\end{aligned} \tag{2}$$

The $(s^\dagger, d^\dagger)$ represents the creation operator, and (s, d) represents the annihilation operator. The parameters $C_L (L = 0, 2, 4)$, $\upsilon (L = 0, 2)$, and $u (L = 0, 2)$ are related to the two-body matrix elements. It is worth noting that the aforementioned equation can also be expressed in multipolar form [4, 21, 22],

$$\hat{H} = \epsilon \hat{n}_d + a_0 \hat{P} \cdot \hat{P} + a_1 \hat{L} \cdot \hat{L} + a_2 \hat{Q} \cdot \hat{Q} + a_3 \hat{T}_3 \cdot \hat{T}_3 + a_4 \hat{T}_4 \cdot \hat{T}_4. \tag{3}$$

The operators are defined as:

$$\left.\begin{aligned} \hat{n}_d &= (d^\dagger \cdot \tilde{d}) \\ \hat{p} &= \frac{1}{2}\left[\left(\tilde{d}\cdot\tilde{d}\right) - (\tilde{s}\cdot\tilde{s})\right] \\ \hat{L} &= \sqrt{10}\left[d^\dagger \times \tilde{d}\right]^1 \\ \hat{Q} &= \left[d^\dagger \times \tilde{s} + s^\dagger \times \tilde{d}\right]^{(2)} + \chi\left[d^\dagger \times \tilde{d}\right]^{(2)} \\ \hat{T}_r &= \left[d^\dagger \times \tilde{d}\right]^{(r)} \end{aligned}\right], \tag{4}$$

where $\hat{n}_d$ is the d-boson operator, $\hat{p}$ is the operator for pairing, $\hat{L}$ is the operator for angular momentum, $\hat{Q}$ is the operator for quadrupole, and $\hat{T}_r$ is the operator for octupole and hexadecapole. The quadrupole structure parameter χ takes on the values 0 and $\pm\frac{\sqrt{7}}{2}$. The parameters ϵ, a_0, a_1, a_2, a_3, and a_4 designate the energy, pairing strength, angular momentum, quadrupole, octupole, and hexadecapole interaction between the bosons.

The U(6) group determines the symmetry of the IBM-1. Its group consists of three subgroups: U(5) for vibration, SU(3) for rotation, and O(6) for soft nuclei [9]:

$$\mathrm{U(6)} \supset \left\{\begin{matrix} \mathrm{U(5)} \supset \mathrm{O(5)} \\ \mathrm{SU(3)} \\ \mathrm{O(6)} \supset \mathrm{O(5)} \end{matrix}\right\} \supset \mathrm{O(2)}. \tag{5}$$

The energy eigenvalues of U(6) subgroups are given by [23]:

$$\left.\begin{aligned} E(n_d, \upsilon, L) &= \epsilon n_d + \beta n_d(n_d+4) + 2\gamma\upsilon(\upsilon+3) + 2\sigma L(L+1) && \mathrm{U(5)} \\ E(\lambda,\mu,L) &= \frac{a_2}{2}(\lambda^2+\mu^2+\lambda\mu+3(\lambda+\mu) + \left(a_1 - \frac{2a_2}{8}\right)L(L+1) && \mathrm{SU(3)} \\ E(\sigma,\tau,L) &= \frac{a_0}{4}(N-\sigma)(N+\sigma+4) + \frac{a_3}{2}\tau(\tau+3) + \left(a_1 - \frac{a_3}{10}\right)(L(L+1)) && \mathrm{O(6)} \end{aligned}\right]. \tag{6}$$

Multiple nuclei have the ability to move between two or more of the previously mentioned boundaries. The behavior of even-even nuclei can be predicted by utilizing the energy ratio $\left(R_{4/2} = \frac{E(4_1^+)}{E(2_1^+)}\right)$ between the first and second low-lying energy levels. Spin, parity,

and level ordering are represented by the symbols in $E(4_1^+)$ and $E(2_1^+)$. Various mathematical expressions, such as SEF [24] and the NEE [25], have been formulated in response to the challenge of studying the nuclear structure, specifically nuclei with deformations. Here is the formula for the SEF used in determining the GSB:

$$E(I) = A_1 \left[e^{A_2 I} - A_3 \right], \tag{7}$$

accordingly, a formula contains three parameters A_1, A_2, and A_3 beside the spin (I). These parameters are determined by fitting, inserting all the experimental energies data in the positive (GSB). Furthermore, γ and β bands can be calculated from the following equation:

$$E(I) = E_0 + (A_1 + B) \left[e^{A_2 I} - A_3 \right], \tag{8}$$

hence, E_0 and B can be estimated from the γ and β bands. Correspondingly, the NEE formula was employed to compute all necessary calculation parameters. The NEE used in determining the GSB:

$$E(I) = \frac{A_1 I(I+1)}{A_2(I+1) + I A_3}, \tag{9}$$

furthermore, γ and β bands can be calculated from the following equation:

$$E(I) = E_0 + \frac{(A_1 + B) I(I+1)}{A_2(I+1) + I A_3}. \tag{10}$$

1.2. The probability of quadrupole transition B(E2)

The electric quadrupole transition can be employed to comprehend the nuclear structure. The $T^{(\mathrm{E2})}$ operator can be employed for the computation of the B(E2) strength [22, 26, 27].

$$B\left((\mathrm{E2}) I_i \to I_f\right) = \frac{1}{2L_i + 1} \left| \langle I_f \parallel T^{(\mathrm{E2})} \parallel I_i \rangle \right|^2, \tag{11}$$

and

$$T^{(\mathrm{E2})} = \alpha_2 \left[d^\dagger \times \tilde{s} + s^\dagger \times \tilde{d} \right] + \beta_2 \left[d^\dagger \cdot \tilde{d} \right] = e_B \hat{Q}, \tag{12}$$

where $e_B = \alpha_2$ is the boson effective charge, and $\beta_2 = \chi\alpha_2$. The electric quadrupole transitions probabilities $B(\mathrm{E2})$ formula is given by [28].

$$B(\mathrm{E2}) = \frac{0.5657}{T_{\frac{1}{2}}\,(\mathrm{ps}) \times E_\gamma^5\,(\mathrm{MeV})}\, e^2\,\mathrm{b}^2 \tag{13}$$

$T_{\frac{1}{2}}$ is the half-time, and E_γ is the transition energy.

1.3. Potential energy surface (PES)

The IBM-1 model is initially explicated in terms of the operators of bosons' creation and annihilation. The state of intrinsic coherence ($|N, \beta, \gamma\rangle$) is expressed as a state of bosons. To produce the coherent state, the boson creation operators (b_c^+) operate on a state of boson vacuum $|0\rangle$ as follows:

$$|N, \beta, \gamma\rangle = \frac{1}{\sqrt{N!}} \left(b_c^\dagger\right)^N |0\rangle, \tag{14}$$

and $\hat{b}_c^\dagger$ is given as:

$$\hat{b}_c^\dagger = \frac{1}{\sqrt{1+\beta^2}} \left\{ s^\dagger + \beta \left[\cos\gamma \left(\hat{d}_0^\dagger \right) + (0.5)^{\frac{1}{2}} \sin\gamma \left(d_2^\dagger + d_{-2}^\dagger \right) \right] \right\}. \tag{15}$$

The PES is defined in terms of β and γ for the purpose of estimating the expected value of the Hamiltonian for the intrinsic boson state [21, 29].

$$E\,(N, \beta, \gamma) = \frac{N\epsilon_d\beta^2}{(1+\beta^2)} + \frac{N(N+1)}{(1+\beta^2)^2} \left[\alpha_1\beta^4 + \alpha_2\beta^3 \cos 3\gamma + \alpha_3\beta^2 + \alpha_4 \right]. \tag{16}$$

The above expression gives (for higher N) $\beta_{\min} = 1, \sqrt{2}$, and 0 for O(6), SU(3), and U(5), respectively. The α_i are related to the coefficients of C_L, v_2, v_0, u_2, and u_0 in Eq. (2).

2. Results and Discussion

The IBM-1, SEF, and NEE framework calculations of the GS, γ, and β bands for $^{170-180}$Os isotopes are discussed below.

For an elementary step in the calculation procedure, the ratio $R_{4/2}$ for each isotope is determined. The $^{170-180}$Os isotopes have dynamical states ranging from U(5) to SU(3), as indicated by the preliminary data in Table 1. It is evident that as the number of neutrons increases, the energy ratio increases very slowly. In addition, Table 2 displays the IBM-1 coefficient values for $^{170-180}$Os isotopes. Tables 3, 4, and 5 exhibit, respectively, the computed GS, β, and γ-band values for the SEF and NEE equations for the investigated isotopes.

Isotopes	Os^{170}	^{172}Os	^{174}Os	^{176}Os	^{178}Os	^{180}Os
$R_{4/2}$	2.615	2.661	2.74	2.92	3.016	3.093

TABLE 1. *$R_{4/2}$ values of Os isotopes*

Isotopes	N	PAIR	ELL	QQ	OCT	α_2	β_2	EPS
^{170}Os	9	0.040	0.045	—	0.02	0.1850	-0.5365	—
^{172}Os	10	0.034	0.014	—	1.04	0.1520	-0.4408	—
^{174}Os	11	0.020	0.046	-0.016	—	0.1450	-0.3330	—
^{176}Os	12	—	0.037	-0.017	—	0.1090	-0.3224	0.13
^{178}Os	13	—	0.038	-0.017	—	0.1047	-0.3098	0.10
^{180}Os	14	—	0.038	-0.017	—	0.0990	-0.2930	—

PAIR $= \frac{a_0}{2}$, ELL $= 2a_1$, QQ $= 2a_2$, OCT $= \frac{a_3}{5}$ [23]

TABLE 2. *IBM-1 data for Os isotopes*

	SEF			NEE		
Isotopes	A_1	$A_2(10^{-3})$	A_3	$A_1(10^{-3})$	A_2	A_3
^{170}Os	5.8452	3.8629	1.0339	7.1041	−0.1939	0.2201
^{172}Os	4.6450	3.8381	1.0324	6.6186	0.0509	0.2232
^{174}Os	1.7464	6.8425	1.0601	3.9020	0.2621	0.0742
^{176}Os	1.3867	8.1450	1.0886	2.9015	0.1383	0.0522
^{178}Os	1.5435	7.7581	1.0925	2.6866	0.0136	0.0657
^{180}Os	1.8224	7.1864	1.0940	2.3835	−0.1599	0.0721

TABLE 3. *GSB results of SEF and NEE for Os isotopes*

		β-band		γ-band	
Isotopes	N	E_0	B	$E_0(10^{-4})$	$B(10^{-4})$
^{170}Os	9	—	—	—	—
^{172}Os	10	-7.1915	-0.8079	-1.0574	0.5425
^{174}Os	11	-2.9848	-0.0451	0.0562	0.0130
^{176}Os	12	-5.9734	-0.9911	0.0607	0.0109
^{178}Os	13	-5.7152	-1.5457	0.0754	0.0040
^{180}Os	14	0.2900	0.0100	0.0642	0.0054

TABLE 4. SEF variables are in MeV for β and γ-bands for Os isotopes

		β-band		γ-band	
Isotopes	N	E_0	B	$E_0(10^{-4})$	$B(10^{-4})$
^{170}Os	9	—	—	—	—
^{172}Os	10	0.6283	0.0478	0.0550	0.0153
^{174}Os	11	0.5210	0.0526	0.0562	0.0129
^{176}Os	12	0.5792	0.0162	0.0607	0.0108
^{178}Os	13	0.6266	0.0096	0.0753	0.0039
^{180}Os	14	0.2900	0.0100	0.0642	0.0054

TABLE 5. NEE variables are in MeV for β and γ-bands for Os isotopes

The Root-Mean-Square-Deviation (RMSD) [30] method was utilized to assess the discrepancy between the energy levels of IBM-1, SEF, and NEE and the empirical data. Table 6 presents RMSD results associated with the three bands. The experimental data [31–36] for the GS, β, and γ bands appeared comparable to

Os	GSB			γ-band			β-band		
Isotopes	IBM-1	SEF	NEE	IBM-1	SEF	NEE	IBM-1	SEF	NEE
^{170}Os	1.1850	1.1816	0.8402	—	—	—	—	—	—
^{172}Os	0.4059	0.0844	0.0060	0.1485	0.0184	0.0178	0.0872	0.2105	0.0938
^{174}Os	0.5799	0.0076	0.0042	0.2481	0.0061	0.0073	0.3438	0.1816	0.0448
^{176}Os	0.4241	0.0115	0.0020	0.0428	0.0037	0.0020	0.0595	0.2204	0.0198
^{178}Os	0.3914	0.0143	0.0013	0.1462	0.0539	0.0603	0.0896	0.0538	0.0216
^{180}Os	0.7553	0.0198	0.0023	0.2121	0.0322	0.0112	0.1226	0.1365	0.1998

TABLE 6. The values of RMSD for the GS, γ and β bands.

the IBM-1, SEF, and NEE computations shown in Figures 1, 2 and 3 respectively. Figure 1 displays the experimental results for GSB, as determined by the IBM-1, SEF, and NEE methods.

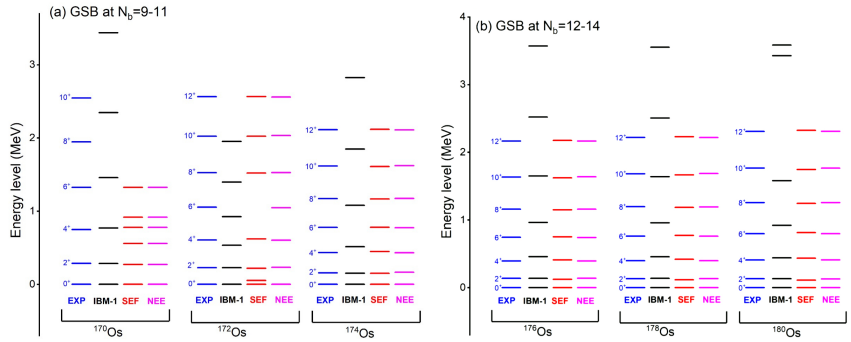

FIGURE 1. *GSB values for the* $170-180$*Os isotopes [31–36]*

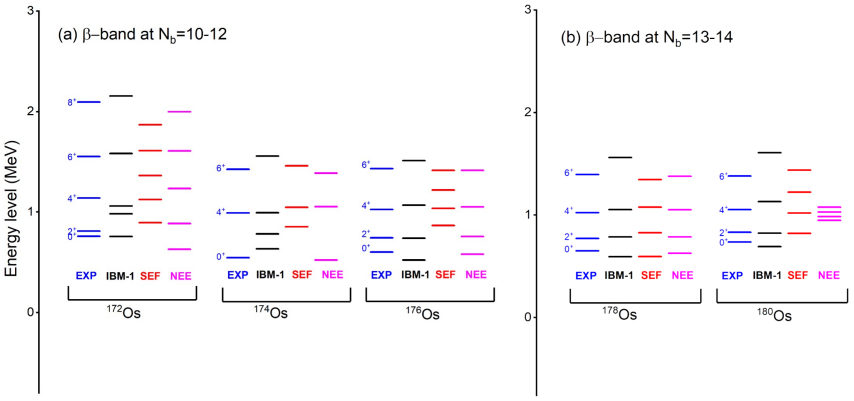

FIGURE 2. *β-band values for the* $170-180$*Os isotopes [31–36]*

The calculated GSB values in SEF, NEE, and IBM-1 exhibit satisfactory agreement with empirical data in certain regions, with the exception of the ^{170}Os isotope calculation, which displays a higher RMSD error. NEE calculations typically exhibit a lower RMSD error compared to SEF and IBM-1 estimations for GSB calculations. IBM-1 calculations for the ^{180}Os isotope revealed a larger error of 75.5 % for the 10^+ state, whereas SEF estimations revealed a maximum error of approximately 8 % for the 2^+ state.

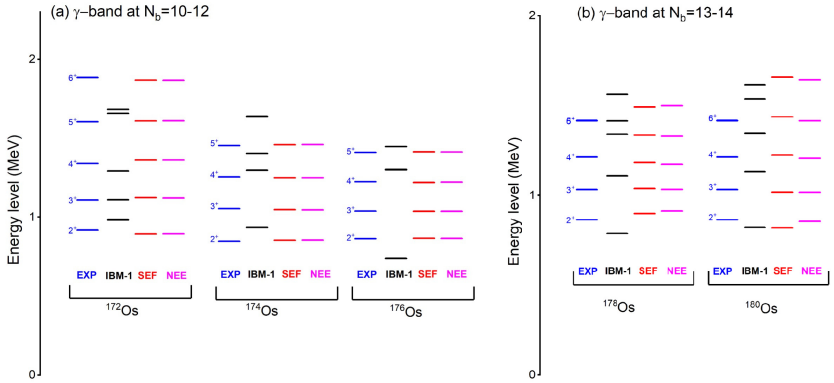

FIGURE 3. *γ-band values for the* $170-180$*Os isotopes [31–36]*

In contrast, NEE has the smallest RMSD error and decreases slightly as excitation energy levels increase. Figure 2 shows that the IBM-1 model has slightly higher RMSD errors for Os isotopes compared to the SEF and NEE estimates for the β-bands. The energy gap between states in the $^{170-180}$Os isotope is equivalent for SEF and NEE calculations. However, for IBM-1 results, it is slightly higher. The NEE calculation for ^{176}Os matches the experimental results exactly, in contrast to the SEF and IBM-1 estimates. The RMSD of ^{176}Os estimates from NEE is smaller than that of SEF and IBM-1. Overall, the SEF, NEE, and IBM-1 calculations accurately reproduced the experimental β-band energy levels. However, discrepancies were observed in the higher states, especially in the IBM-1 calculations. Furthermore, the NEE calculation for ^{180}Os fails to properly represent the energy level when compared to experimental data or other calculations.

The RMSD error value in the IBM-1 calculations for $^{170-180}$Os isotopes is higher compared to SEF and NEE estimations for the γ-band, as shown in Figure 3. Based on empirical data, the disparity between the energy levels of the Os isotope is similar for SEF and NEE, but more significant for IBM-1. The NEE and SEF calculations exhibit a perfect agreement with the experimental data when compared to the IBM-1 calculations. The average error in calculating NEE for all Os isotopes is smaller compared to SEF and

$I_i \to I_f$	^{170}Os		^{172}Os		^{174}Os	
	IBM-1	Exp.	IBM-1	Exp.	IBM-1	Exp.
$2_1^+ \to 0_1^+$	0.8009	———	0.6469	0.653	0.9952	———
$2_2^+ \to 0_1^+$	0.1078	———	0.0867	———	0.0045	———
$2_3^+ \to 0_1^+$	———	———	———	———	0.0001	———
$4_1^+ \to 2_1^+$	1.0952	———	0.8912	0.981	1.3957	0.9822
$4_2^+ \to 2_1^+$	0.0844	———	0.0692	———	0.0028	———
$4_3^+ \to 2_1^+$	———	———	———	———	0.0001	———
$6_1^+ \to 4_1^+$	1.1979	———	0.9858	1.705	1.4858	———
$6_2^+ \to 4_1^+$	0.0628	———	0.0529	———	0.0023	———
$6_3^+ \to 4_1^+$	———	———	———	———	0.0001	———
$8_1^+ \to 6_1^+$	1.1948	———	0.9998	2.159	1.4776	———
$8_2^+ \to 6_1^+$	0.0446	———	———	———	0.0021	———
$8_3^+ \to 6_1^+$	———	———	0.0392	———	———	———
$10_1^+ \to 8_1^+$	1.1189	———	0.9597	1.477	1.4135	———
$10_2^+ \to 8_1^+$	0.0297	———	———	———	0.0018	———
$10_3^+ \to 8_1^+$	———	———	0.0278	———	———	———
$12_1^+ \to 10_1^+$	0.9857	———	0.8780	1.591	1.3078	———
$12_2^+ \to 10_1^+$	———	———	———	———	0.0015	———
$12_3^+ \to 10_1^+$	0.0179	———	0.0185	———	———	———

TABLE 7. Theoretical and experimental B(E2) values in e^2b^2 unit for the $^{170-174}$Os isotopes.[31–33]

IBM-1. The SEF and NEE values for ^{170}Os could not be calculated because there is a lack of experimental data for the β and γ bands. Furthermore, Tables 7, and 8 present a comparative analysis of the B(E2) result obtained from experimental and calculated data for all the nuclei being examined. Most results derived from IBM-1 exhibit coherence with the results that can be obtained, except for higher excited energy levels. The reason behind this is that the IBM-1 is successful in explaining low-lying energy levels, but its results are far from satisfactory for higher-excited levels.

Finally, the transitional region SU(3)-O(6) in the parameter space of two control variables, β and γ, was investigated in this study. If $\beta = 0$, the shape is spherical, while for $\beta \neq 0$, the shape is deformed.

$I_i \to I_f$	^{176}Os		^{178}Os		^{180}Os	
	IBM-1	Exp.	IBM-1	Exp.	IBM-1	Exp.
$2_1^+ \to 0_1^+$	0.7374	———	0.8096	0.8250	0.8510	0.849
$2_2^+ \to 0_1^+$	0.0015	———	0.0008	———	———	———
$2_3^+ \to 0_1^+$	0.0013	———	0.0006	———	———	———
$4_1^+ \to 2_1^+$	1.0385	———	1.1417	———	1.2017	1.159
$4_2^+ \to 2_1^+$	0.0014	———	0.0008	———	———	———
$4_3^+ \to 2_1^+$	0.0006	———	0.0003	———	———	———
$6_1^+ \to 4_1^+$	1.1139	———	1.2279	———	1.2958	0.966
$6_2^+ \to 4_1^+$	0.0009	———	0.0006	———	———	———
$6_3^+ \to 4_1^+$	0.0005	———	0.0002	———	———	———
$8_1^+ \to 6_1^+$	1.1203	———	1.2405	———	1.3144	0.380
$8_2^+ \to 6_1^+$	0.0006	———	0.0004	———	———	———
$8_3^+ \to 6_1^+$	0.0003	———	0.0002	———	———	———
$10_1^+ \to 8_1^+$	1.0884	———	1.2137	———	1.2937	———
$10_2^+ \to 8_1^+$	0.0003	———	0.0003	———	———	———
$10_3^+ \to 8_1^+$	0.0002	———	0.0002	———	———	———
$12_1^+ \to 10_1^+$	1.0282	———	1.1589	———	1.2457	———
$12_2^+ \to 10_1^+$	0.0002	———	0.0002	———	———	———
$12_3^+ \to 10_1^+$	0.0002	———	0.0001	———	———	———
$14_1^+ \to 12_1^+$	0.9440	———	1.0809	———	1.1759	———
$14_2^+ \to 12_1^+$	0.0001	———	0.0001	———	———	———
$14_3^+ \to 12_1^+$	0.0001	———	0.0001	———	———	———
$16_1^+ \to 14_1^+$	0.8377	———	0.9823	———	1.0868	———
$16_2^+ \to 14_1^+$	———	———	———	———	———	———
$16_3^+ \to 14_1^+$	———	———	———	———	———	———
$18_1^+ \to 16_1^+$	0.7104	———	0.8642	———	0.9799	———
$18_2^+ \to 16_1^+$	———	———	———	———	———	———
$18_3^+ \to 16_1^+$	———	———	———	———	———	———
$20_1^+ \to 18_1^+$	0.5626	———	0.7274	———	0.8563	———
$20_2^+ \to 18_1^+$	———	———	———	———	———	———
$20_3^+ \to 18_1^+$	———	———	———	———	———	———
$22_1^+ \to 20_1^+$	0.3949	———	0.5723	———	0.7163	———
$22_2^+ \to 20_1^+$	———	———	———	———	———	———
$22_3^+ \to 20_1^+$	———	———	———	———	———	———
$24_1^+ \to 22_1^+$	0.2072	———	0.3993	———	1.0684	———
$24_2^+ \to 22_1^+$	———	———	———	———	———	———

TABLE 8. Theoretical and experimental B(E2) values in e^2b^2 unit for the $^{176-180}$Os isotopes.[34–36]

The value of γ represents the degree of deviation from the focus symmetry that is associated with the nucleus. A value of $\gamma = 0$ indicates a prolate shape; $\gamma = \pi/3$ indicates an oblate shape; and $0\ \gamma \leq \pi/3$ indicates a triaxial shape. The potential energy surface for the even-even $^{170-180}$Os isotopes is depicted in Figure 4. The presented figure illustrates the transition of the shape phase from rotational SU(3) to γ-unstable symmetry O(6) in $^{170-180}$Os isotopes ($\pi/6 \leq \gamma \leq \pi/3$).

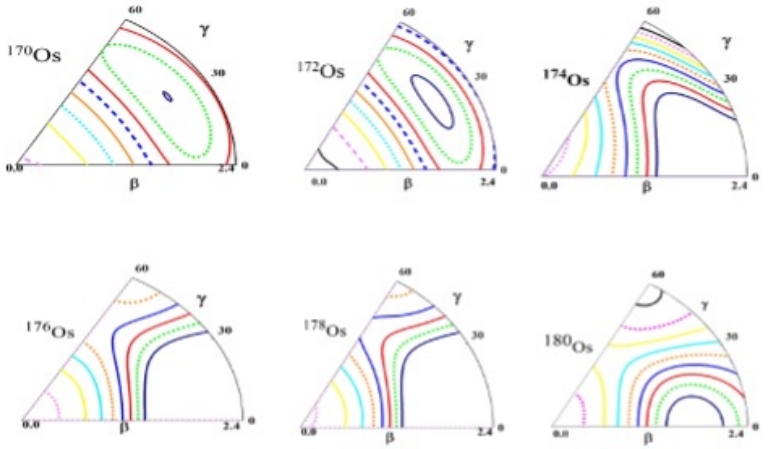

FIGURE 4. *Surface maps of potential energy for the* $170-180\,Os$ *isotopes[31–36]*

Conclusions

Current research used IBM-1, SEF, and NEE approaches to determine the energy states of the ground state (GS), β, and γ-bands in the $^{170\text{-}180}$Os isotopes. The results of the study in relation to the GS, β, and γ bands indicate that IBM-1, SEF, NEE, and available experimental data exhibit a degree of agreement, but with some discrepancies. Furthermore, the NEE results related to GS, β, and γ bands exhibit greater conformity with empirical results in comparison to the estimations derived from IBM-1 and SEF models. In addition, the reduced transition probabilities B(E2) of the IBM-1 model match the experimental data well. The analysis of potential energy surfaces for $^{170\text{-}180}$Os isotopes reveals that

these isotopes exhibit deformation and are classified within the SU(3)-O(6) symmetry group. In the IBM-1 model, the energies of the 6^+, 8^+, and 10^+ states are not accurately represented, especially in the GS bands. Additionally, as the number of neutrons increases, the $R_{4/2}$ values of low-lying energy levels of Os isotopes vary gradually.

Acknowledgments

The authors convey their appreciation to the University of Mosul, College of Education for Pure Sciences, Department of Physics, for their support in carrying out this research.

References

[1] T. Otsuka, A. Arima, and F. Iachello, Nucl. Phys. A **309**, 1 (1978).

[2] W. Greiner and J. Reinhardt, *Field Quantization* (Springer Berlin, Heidelberg, 1996).

[3] F. Pan and J. Draayer, Nucl. Phys. A **636**, 156 (1998).

[4] A. Arima and F. Iachello, Ann. Phys. **99**, 253 (1976).

[5] F. Iachello and A. Arima, Phys. Lett. B **53**, 309 (1974).

[6] A. Arima and F. Iachello, Phys. Rev. Lett. **35**, 1069 (1975).

[7] P. Cejnar, J. Jolie, and R. F. Casten, Rev. Mod. Phys. **82**, 2155 (2010).

[8] R. Kumar, S. K. Sharma, and J. B. Gupta, Armen. J. Phys. **3**, 150 (2010).

[9] A. M. Al-Nuaimi, R. Alkhayat, and M. Al-Jubbori, Karbala Int. J. Mod. Sci. **8**, 391 (2022).

[10] W. Zhang, B. Cederwall, and et al., Phys. Lett. B **820**, 136527 (2021).

[11] A. Goasduff, J. Ljungvall, and et al., Phys. Rev. C **100**, 034302 (2019).

[12] P. H. Regan, C. W. Beausang, and et al., Phys. Rev. Lett. **90**, 152502 (2003).

[13] D. Bonatsos, P. E. Georgoudis, and et al., Phys. Rev. C **88**, 034316 (2013).

[14] J. B. Gupta and S. Sharma, Indian J. Pure Appl. Phys. **26**, 601 (1988).

[15] M. A. Al-Jubbori, H. H. Kassim, and et al., Nucl. Phys. A **970**, 438 (2018).

[16] K. Nomura, T. Otsuka, and et al., Phys. Rev. C **84**, 054316 (2011).

[17] I. Hossain, H. H. Kassim, and et al., ScienceAsia **42**, 22 (2016).

[18] M. Délèze, S. Drissi, and et al., Nucl. Phys. A **551**, 269 (1993).

[19] H. El-Gendy, Nucl. Phys. A **1006**, 122117 (2021).

[20] A. Mohammed-Ali, R. B. Alkhayat, and et al., Rev. Mex. Fis. **68**, 060401 (2022).

[21] A. E. L. Dieperink, O. Scholten, and F. Iachello, Phys. Rev. Lett. **44**, 1747 (1980).

[22] R. F. Casten, *The Interacting Boson Approximation Model*, International School of Physics Enrico Fermi, Vol. 169 (IOS Press, 2008) p. 385.

[23] R. F. Casten and D. D. Warner, Rev. Mod. Phys. **60**, 389 (1988).

[24] M. A. Al-Jubbori, H. H. Kassim, and et al., Nucl. Phys. A **955**, 101 (2016).

[25] M. A. Al-Jubbori, F. S. Radhi, and et al., Nucl. Phys. A **971**, 35 (2018).

[26] H. H. Kassim, A. A. Mohammed-Ali, and et al., Iran. J. Sci. Technol., Trans. Sci. **42**, 993 (2018).

[27] S. M. Mutsher, F. I. Sharrad, and E. A. Salman, Nucl. Phys. A **1017**, 122342 (2022).

[28] S. Raman, C. Nestor, and P. Tikkanen, Atom. Data Nucl. Data **78**, 1 (2001).

[29] K. Abrahams, K. Allaart, and A. E. L. Dieperink, *Nuclear Structure*, Vol. 67 (Springer New York, NY, 2012).

[30] F. X. Xu, C. S. Wu, and J. Y. Zeng, Phys. Rev. C **40**, 2337 (1989).

[31] E. Browne and H. Junde, Nucl. Data Sheets **87**, 15 (1999).
[32] M. Basunia, Nucl. Data Sheets **107**, 791 (2006).
[33] C. Baglin, E. McCutchan, and et al., Nucl. Data Sheets **153**, 1 (2018).
[34] E. Achterberg, O. Capurro, and G. Marti, Nucl. Data Sheets **110**, 1473 (2009).
[35] E. McCutchan, Nucl. Data Sheets **126**, 151 (2015).
[36] B. Singh, Nucl. Data Sheets **96**, 1 (2002).